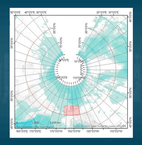

A Deep Learning-Based Approach for Mapping Tall Shrubs in Arctic Tundra

Darko Radakovic[1], Mark Chopping[1], Rocio Duchesne[2], Angela Erb[3], Zhuosen Wang[4] and Crystal Schaaf[3]

[1] Montclair State University [2]University of Wisconsin Whitewater [3]University of Massachusetts, Boston [4]University of Maryland CP/ESSIC

Objectives We aim to improve the mapping and quantify tall shrubs in the Arctic, using machine learning (ML) techniques over a period of ~10-18 years to assess changes in (tall) shrub succession in northern Alaska. The objective of this study is to employ semi-automated techniques to analyze high resolution (<1 m) images taken by satellites in orbit to evaluate variations in the growth of shrubs in numerous locations across the Arctic tundra regions of Alaska and Canada, spanning a decade to a decade and a half. The data produced were intended to be accessible to ABoVE researchers for evaluating the effects on summer terrestrial albedo, comparing changes in shrub abundance in Arctic tundra from the satellite high resolution record and albedo, verifying lower spatial resolution ABoVE remote sensing data products, and initiating, driving, calibrating and validating ecological models.

Imagery The project leveraged the availability of commercial high spatial resolution satellite imagery, including QuickBird (~ 0.6 m) from around 2005 and WorldView-2 (~0.4 m) and WorldView-3 (~0.3 m) from around 2013 to 2022, for diverse cloud-free, summer tundra landscapes. The Maxar Technologies (then DigitalGlobe) catalog is available to NASA Earth Science investigators, at the NASA Center for Climate Simulation (NCCS).

Study domain

Models Yolov8 (released Jan. 2023) model (You only Look Once) was used for object detection of individual shrubs and segmentation to identify diverse tundra landscape patches,. such as dense tall shrub areas and polygonal ground in the satellite images (figure 1). The models are open sourced and accessible with Python.

Training 2-by-2 km areas were chosen across the study domain. Sub-areas of 100 m from Pansharpened QuickBird and WorldView were used for training with two different techniques were used for annotating shrubs: 1) Object detection with bounding boxes and 2) Segmentation with polygons. The dataset was divided in train (70%), validation (20%) and test (10%) sets. Based on the type of annotation, the ML-model was chosen (figure 2). A relatively small training and validation sets were used for various experiments aiming to improve the mean Average Precision (mAP), e.g., comparing subset area size, object detection vs segmentation and image quality. Our experimental models showed that the mAP was larger for pansharpened imagery compared to panchromatic imagery. Furthermore, augmentation (tilting, cropping and rotation of the input images) and resizing to 640x640 pixels improved the accuracy of the model. Segmentation was most accurate with NASA's Goddard's Lidar, Hyperspectral and Thermal (G-LiHT) data (figure 3).

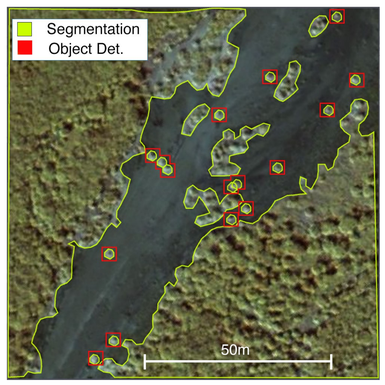

Figure 1. Example of Segmentation and Object detection annotations for a sample site in Alaska QuickBird (QB) Aug 4, 2004 imagery near the Colville River, North Slope, Alaska (Maxar, 2004: QB02_20040804220230_1010010003255300_04AUG04220230-P1BS-500537153040_01_P001)

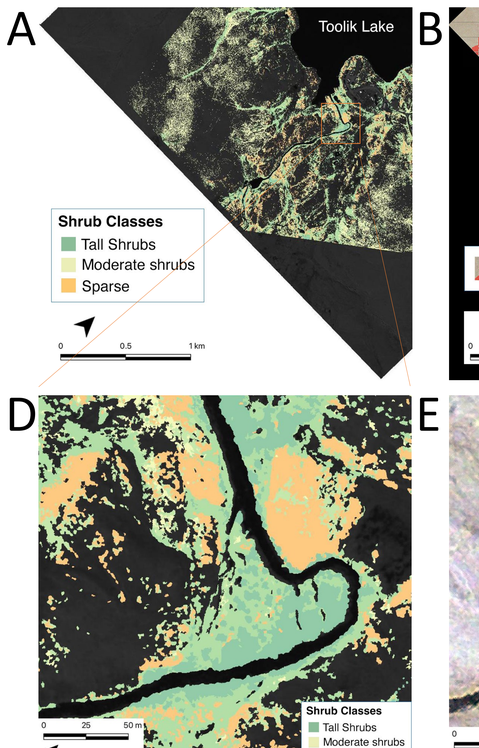

Figure 4. Toolik lake site in Alaska (a) Vegetation Community Map, Toolik Lake Area, Alaska, 2013-2015 (Greaves et al. 2018) (b) Segmentation detections shrub patches pan-sharpened QuickBird (QB), Aug 4, 2004 (Maxar, 2004: QB02_20040804220250_1010010003255300_04AUG04220250-P1BS-500537153040_01_P007) (c) Segmentation detections shrub patches pan-sharpened WorldView-2 (WV02), June 16, 2012 (Maxar, 2016: WV02_20160612215015_1030010057A6E600_16JUN12215015-P1BS-501511474060_01_P012) (d) Close up of Vegetation Community Map at the Toolik site (e) Close up of pansharpened QuickBird at the Toolik site (f) Close up of object detections of (tall) shrubs (in blue) on the pansharpened QuickBird at the Toolik site without a Convolution Neural Network Filter applied.

Calibration All imagery was orthorectified to the ABoVE Albers Conic Equal Area (Canada) grid (0.5 m) and converted to calibrated spectral radiances using the Polar Geospatial Center's pgc_ortho.py code and Alaska DEM (alaskaned_mosaic_wgs84). In addition, fine-tuning of the output grid upper left XY was needed to match the Toolik Lake Vegetation Community Map.

Validation The accuracy of ML-generated maps was checked using the fine resolution (± 0.02m) Vegetation Community Map, Toolik Lake Area, Alaska, 2013-2015," which were created using high resolution UAS imagery and lidar data (Greaves et al. 2018).

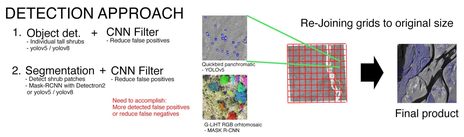

Figure 2. ML annotation approach with Object and Segmentation techniques.

Results Object detection of individual shrubs and segmentation of shrub patches for both QuickBird and WorldView images was compared to the Vegetation Community Map, Toolik Lake Area seen in Table 1 and figure 4. Shrub patches with Segmentation in QuickBird and WorldView images produces lower accuracies compared to object detection. Object detection on the other hand has a low recall, due to the few detections when compared with the Vegetation community map. However, most of the predicted labels are correct when compared to the training labels. F1-scores are low for all detections which could indicate that the detected classes are imbalanced. NDVI vegetation cover maps were used to determine the relationship with ML object detection confidence (figure 4). Water depth and tundra landscape type can be related to shrub cover (fig 5.).

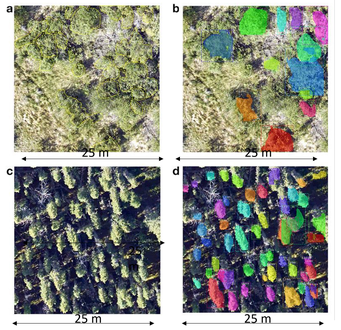

Figure 3. MASK-RCNN Segmentation detections on shrubs (a,b) and trees (c,d) on fine-scale (~0.02m) G-LiHT Orthomosaic RGB 25 m subsets in Alaska, Jul. 2018 (south of North Slope).

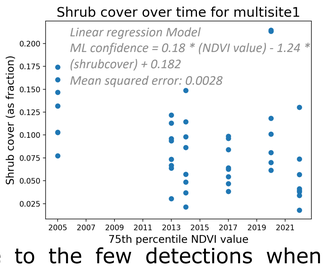

Figure 4. Extracting NDVI mean values from images to better determine the specific confidence level of the ML detection model can help improve a more valid result

TABLE 1. TALL SHRUB MEASUREMENT RESULTS, BEST RUNS

	Confidence	Precision	Recall	Accuracy	F1-Score
SEGMENTATION on QB 100m PSHP	0.1				
all classes		0.31	0.29	0.58	0.15
sparse		0.1	0.12	0.47	0.05
moderate		0.07	0.09	0.47	0.04
tall shrubs		0.02	0.03	0.45	0.01
SEGMENTATION on QB 100m PSHP	0.2				
all classes		0.42	0.32	0.6	0.18
sparse		0.13	0.12	0.54	0.06
moderate		0.12	0.1	0.54	0.05
tall shrubs		0.04	0.03	0.54	0.02
SEGMENTATION on WV 100m PSHP	0.1				
all classes		0.52	0.34	0.6	0.21
sparse		0.19	0.13	0.58	0.08
moderate		0.15	0.1	0.6	0.06
tall shrubs		0.05	0.03	0.62	0.02
SEGMENTATION on WV with CNN filter	0.1				
all classes		0.56	0.24	0.67	0.17
sparse		0.25	0.1	0.69	0.07
moderate		0.19	0.08	0.71	0.06
tall shrubs		0.06	0.02	0.74	0.01
SEGMENTATION on WV 100m PSHP	0.2				
all classes		0.52	0.35	0.6	0.21
sparse		0.18	0.13	0.58	0.08
moderate		0.16	0.11	0.59	0.07
tall shrubs		0.05	0.03	0.61	0.02
Object Detection on QB 100m PSHP	0.1				
all classes		0.97	0.37	0.63	0.27
sparse		0.89	0.16	0.83	0.14
moderate		0.82	0.1	0.88	0.09
tall shrubs		0.55	0.03	0.95	0.03
Object Detection on QB WITH CNN	0.1				
all classes		0.97	0.37	0.63	0.27
sparse		0.89	0.16	0.83	0.14
moderate		0.83	0.1	0.88	0.09
tall shrubs		0.56	0.03	0.95	0.03
Object Detection on QB 100m PSHP	0.2				
all classes		0.99	0.38	0.62	0.27
sparse		0.95	0.16	0.84	0.14
moderate		0.93	0.11	0.89	0.1
tall shrubs		0.78	0.03	0.96	0.03
Object Detection on QB with CNN	0.2				
all classes		1	0.38	0.62	0.28
sparse		1	0.16	0.84	0.14
moderate		1	0.11	0.89	0.1
tall shrubs		1	0.03	0.97	0.03

Findings and Future Work Assessing changes in shrub cover and biomass using high resolution imagery relies not only on precise detections, but also on the numbers (recall), which can be affected by training data. Imprecision can be reduced by utilizing Convolution Neural Network (CNN) filters to reduce false positives, however, further testing with imagery from other regions is necessary to determine the ML strategy. Image variations (e.g., between QB and WV, sun angle etc.) challenge a one-to-all algorithm approach. Extracting NDVI mean values to better determine the specific confidence level of the ML detection model can help improve a more valid result

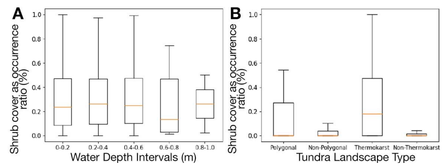

Figure 5. Combining shrub cover with water depth (A) level and landscape type (B)

NASA Award NNX15AU08A

Acknowledgments: We gratefully acknowledge the assistance of the NASA, GSFC NCCS User Services Group (support@nccs.nasa.gov); Liz Hoy (ABoVE Science Cloud Lead, NASA, GSFC); Mark Carroll (NASA, GSFC); Clare Porter (Polar Geospatial Center); Jim Shute (NASA Center for Climate Simulation (NCCS)); Bruce Cook (NASA Goddard Space Flight Center); NASA Center for Climate Simulation (NCCS); ©2004, 2016 Maxar Technologies.

References

Cook, B. D., L. W. Corp, R. F. Nelson, E. M. Middleton, D. C. Morton, J. T. McCorkel, J. G. Masek, K. J. Ranson, V. Ly, and P. M. Montesano. (2013). NASA Goddard's Lidar, Hyperspectral and Thermal (G-LiHT) airborne imager. Remote Sensing 5:4045-4066, doi:10.3390/rs508404

Greaves, H.E., L. Vierling, J. Eitel, N. Boelman, T. Magney, C. Prager, and K. Griffin. 2018. High-Resolution Shrub Biomass and Uncertainty Maps, Toolik Lake Area, Alaska, 2013. ORNL DAAC, Oak Ridge, Tennessee, USA. https://doi.org/10.3334/ORNLDAAC/1573

MONTCLAIR STATE UNIVERSITY